

Bistability in a simple fluid network due to viscosity contrast

John B. Geddes*

*Franklin W. Olin College of Engineering, Needham MA and
Institute for Complex Systems and Mathematical Biology, University of Aberdeen, Scotland*

Brian D. Storey and David Gardner

Franklin W. Olin College of Engineering, Needham MA

Russell T. Carr

Department of Chemical Engineering, University of New Hampshire, Durham NH

(Dated: June 3, 2022)

We study the existence of multiple equilibrium states in a simple fluid network using Newtonian fluids and laminar flow. We demonstrate theoretically the presence of hysteresis and bistability, and we confirm these predictions in an experiment using two miscible fluids of different viscosity—sucrose solution and water. Possible applications include bloodflow, microfluidics, and other network flows governed by similar principles.

Introduction—The control of and exploitation of fluids in channels on the order of ten to one hundred microns has numerous applications, particularly in biology and medicine [1]. Although flows on this scale are typically laminar and are dominated by viscosity, the small volumes involve physics not usually seen on the macroscale [2]. In the last ten years, multiple researchers have demonstrated that microfluidic memory, logic, and control devices can be constructed using a single-phase fluid with elastic properties [3, 4] or using droplets or bubbles which form spontaneously when two immiscible fluids merge [5, 6, 7]. The flow of droplets through microfluidic networks also demonstrates classical nonlinear phenomena such as bistability, periodic, and aperiodic oscillations, even when the network boundary conditions are fixed [8, 9]. The source of nonlinearity in this case is the hydrodynamic resistance due to the presence of droplets in various parts of the network [10]. These recent studies are reminiscent of classic fluidic circuits which were quite common in the 1960s [11]. In classic fluidics the nonlinearity needed to build devices such as logic gates and flip-flops comes from inertial flow effects, which is not present in microfluidic systems.

Another important fluid network on the same scale is the microvascular network, which has also come under increased scrutiny in the last decade. The flow of blood through networks of small vessels is of critical importance in maintaining healthy tissue and, in conjunction with vascular remodeling, may be responsible for diseases like hypertension [12]. There is also a growing body of evidence that the structure and flow properties of tumor vasculature may play a key role in the efficacy of drug treatment for cancer [13]. Modeling and simulation of microvascular bloodflow involves a number of rheological effects that are absent in larger vessels (see [14] for a good review). The Fahraeus-Lindqvist effect refers to the viscosity of blood as a function of both hematocrit (red blood cell volume concentration) and vessel diameter. The apparent reduction in viscosity as diameter decreases is usually attributed to the existence of a lubricating layer of plasma along the edge of the vessel. This lubricating layer is also responsible for the plasma skimming effect which describes the flow-dependent separation of blood at diverging bifurcations. In microvessels, the red blood cell flow differs from the total flow. Downstream vessels which receive more total flow receive an even higher red blood cell flow and vice versa. Numerous investigators have characterized and parametrized these effects both *in vivo* and *in vitro* [15]. While key for properly capturing the details of blood flow in small vessels, these effects also apply to other concentrated suspensions.

Over the last ten years, we (JBG and RTC) have focused our attention on analyzing the flow of blood through small networks of microvessels. We have demonstrated that, in a simple network consisting of a single inlet, a loop, and a single outlet multiple equilibria could exist and that steady state solutions could become unstable via a Hopf bifurcation to a limit cycle oscillation [16, 17]. We proved that the Fahraeus-Lindqvist effect and the plasma skimming effect were necessary, but not sufficient, for the existence of multiple equilibria and limit cycle oscillations—the Fahraeus-Lindqvist effect and plasma skimming effect must be sufficiently “strong”. Our analysis to date indicates that blood is too weakly nonlinear for multiple equilibria and limit cycle oscillations to be observable in this simple two-node microvascular network. Oscillations have been observed, however, in an identical two-node network with a flow of droplets [8]. In this case the droplets enter the branch that gets most of the flow which corresponds to the winner-take-all plasma skimming case.

More recently, we have turned our attention to the three-node network (Figure 1) which consists of two inlets, a

*Address correspondence to:john.geddes@olin.edu

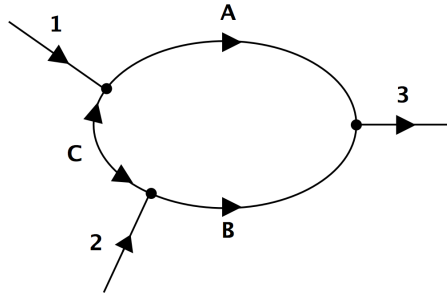


FIG. 1: Water enters feed vessel 1 and a water-sucrose mixture enters feed vessel 2. The network can either be flow-driven or pressure-driven. The flow in vessel C can be either clockwise or counter-clockwise depending on the equilibrium flow distribution.

loop, and one outlet. The flow in vessel C can be clockwise or counter-clockwise depending on the equilibrium state. Using models of the Fahraeus-Lindqvist effect and the plasma skimming effect appropriate for *in vivo* bloodflow [15], we have demonstrated that realistic network geometries exist which can support flow in either direction in vessel C, i.e. bistability. We were surprised to discover, however, that these results are robust even for large vessels in which plasma skimming is negligible. This suggests then that a nonlinear viscosity may be sufficient to observe bistability in this simple three-node network. In this paper, we experimentally demonstrate bistability using two simple miscible fluids—water in feed vessel 1 and a water-sucrose mixture in feed vessel 2. After reviewing the model and the theoretical predictions we discuss the experimental set-up and present results which confirm our analysis. We end with a discussion of the implications of these results.

Model—We explore the behavior of flow in the simple three-node network shown in Figure 1. Two miscible fluids of different viscosities are injected in inlet 1 and 2. The network model assumes laminar, fully developed flow in each of the vessels with well-mixed fluid after junctions where the two fluids meet. Similar results can be obtained even if the fluids do not mix after junctions, but we do not consider that case here.

The resistance, R , of each tube provides the relationship between pressure drop and flow rate;

$$\Delta P = RQ = \frac{128\mu L}{\pi D^4} Q, \quad (1)$$

where ΔP is the pressure drop across the vessel, D is the diameter, L is the length, μ is the viscosity, and Q is the volumetric flow rate. The total pressure drop around the loop must be zero,

$$\Delta P_A = \Delta P_B + \Delta P_C, \quad (2)$$

where ΔP_A and ΔP_B are positive with the flow toward the exit. While the direction of the flow in vessel C may be in either direction, we define ΔP_C to be positive when the flow is counter-clockwise, i.e. from inlet 1 to inlet 2. Since the liquid is incompressible the total flow rate into any junction must also equal the flow rate out, namely $Q_A = Q_1 - Q_C$ and $Q_B = Q_2 + Q_C$. When the fluids mix at a node, their volumes are additive such that we can compute the volume fraction of fluid 2, ϕ , in the resulting mixture. Using this volume fraction to characterize the mixture composition means that $\phi_1 = 0$ and $\phi_2 = 1$. When Q_C is positive (from inlet 1 to inlet 2)

$$\phi_A = 0, \quad \phi_B = \frac{Q_2}{Q_C + Q_2}, \quad \phi_C = 0. \quad (3)$$

When Q_C is negative (from inlet 2 to inlet 1),

$$\phi_A = \frac{Q_C}{Q_C - Q_1}, \quad \phi_B = 1, \quad \phi_C = 1. \quad (4)$$

The viscosity of the mixture can be captured using a modified Arrhenius law,

$$\log(\mu) = (1 - N)\log(\mu_1) + N\log(\mu_2) + N(1 - N)d, \quad (5)$$

where N is the mole fraction of fluid 2 and d is a fit parameter. The first two terms on the right hand side are the classic Arrhenius law and third term is an empirical correction factor [18]. We use this relationship to fit experimental data for mixtures [19].

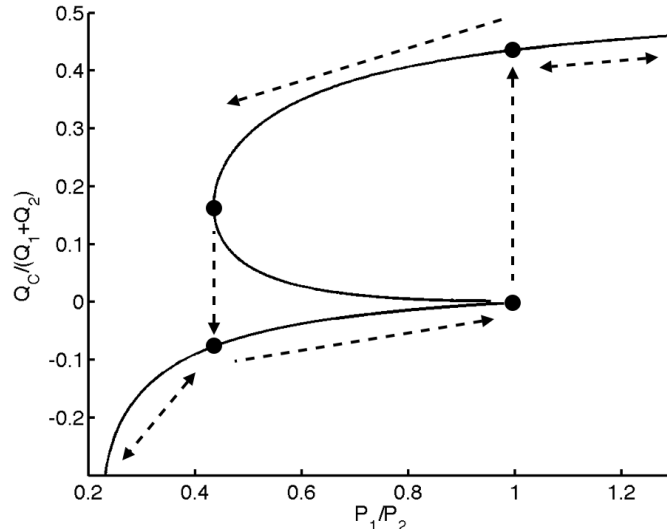


FIG. 2: Normalized flow rate in branch C as a function of the pressure ratio for a sucrose concentration (by volume) in vessel 2 of 0.55 and the parameter values defined in the text. The flow is bistable between the two switching points which can be measured experimentally.

Using Eq. 2 and the conservation of flow, the flow in C can be expressed in terms of the inlet flow in 1 and 2,

$$Q_C = \frac{Q_1 R_A - Q_2 R_B}{R_A + R_B + R_C}. \quad (6)$$

In this way, Eqs. (3)-(6) define a nonlinear, algebraic equation for the flow in vessel C which is parameterized by the inlet flows, the viscosity ratio between the fluids, and the length and diameter of the vessels. It is possible to find network parameters, i.e. vessel lengths, diameters, and inlet fluid viscosities such that the equilibrium flow in vessel C demonstrates hysteresis or bistability as the inlet flow rates are varied.

In our experiments we drive the network by applying fixed pressure at inlet 1 and 2 and the exit 3. This setup is a matter of convenience as it is very simple and reliable to use gravity to apply a known pressure. Under pressure-driven conditions, Eqs. (6)-(4) are supplemented with equations for the inlet pressures relative to the exit pressure,

$$P_1 = (Q_1 + Q_2)R_3 + (Q_1 - Q_C)R_A + Q_1 R_1, \quad (7)$$

$$P_2 = (Q_1 + Q_2)R_3 + (Q_2 + Q_C)R_B + Q_2 R_2. \quad (8)$$

Under pressure-driven conditions the resistance of the inlet and outlet vessels enters the formulation. We can prove that if the equilibrium flow in vessel C demonstrates bistability through Eqs. (3)-(6), bistability will be observed under pressure-driven conditions.

In Figure 2 we plot a sample equilibrium curve as a function of the inlet pressure ratio using the following parameter values: $D_A = D_B = D_C = D_1 = D_2 = D_3$, $L_A = L_B$, $L_C = \frac{6}{45}L_B$, $L_1 = L_2 = L_3 = \frac{4}{15}L_B$, $\mu_2/\mu_1 = 28$. For relatively low pressure ratios (i.e. $P_2 \gg P_1$), Q_C is negative (from inlet 2 to inlet 1). As the pressure ratio is increased the flow in C slows to zero and then suddenly switches direction such that Q_C is positive. For the chosen parameter values the critical pressure ratio at which switching occurs is $P_1/P_2 = 1$ because the network is symmetric. Decreasing the inlet pressure ratio from this point results in Q_C remaining positive, thus demonstrating bistable behavior. As the inlet pressure ratio is further decreased, the flow in Q_C spontaneously switches direction again and travels once more from inlet 2 to inlet 1. These switching points are observed experimentally.

Experiments—In order to test the prediction of bistability, we built a simple and inexpensive experimental flow network. The flow network was constructed with common 1/16 inch inner diameter clear plastic tubing. The connections in the network are made with barbed T fittings. In order to have well-mixed flow in the vessels, we place static inline flow mixers right after the T-junctions in vessels A and B. Without the mixers, the two fluids remain stratified (they were not density matched) which changes the switching points but does not destroy the hysteresis.

Inlet vessels 1 and 2 are connected to a pressure source, which is simply a large graduated cylinder filled to a set level. The graduated cylinders act as our flow reservoirs and the pressure of the reservoirs are known from hydrostatics. The reservoir levels change slowly as the network drains, but this draining can be offset by slowly pumping new fluid

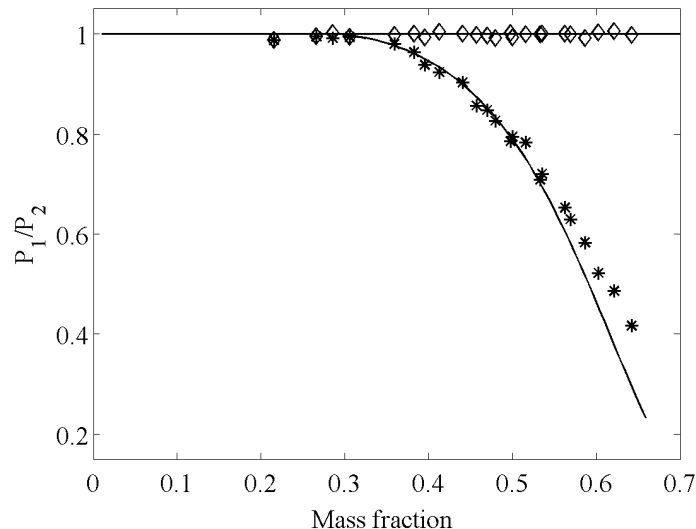


FIG. 3: Switching pressures versus mass fraction of sucrose in inlet 2 as determined experimentally (points) and predicted by the model (lines). Below a concentration of approximately 30% no bistable behavior is expected nor observed.

into the reservoirs. Inlet 1 always contains pure deionized water while inlet 2 consists of an aqueous sucrose solution of varying concentration. Food coloring is added so that we can observe the direction of flow in vessel C as well as confirm mixing in the vessels. The relative vessel lengths were chosen as described previously with $L_B = 0.75\text{m}$. The mixers were tested experimentally and their equivalent resistance was approximately that of 0.375m of additional tubing. Before each experiment, we measure the viscosity and density of the sucrose mixture in reservoir 2 to confirm that it matches known data [19].

To observe bistability, the level of the sucrose solution in reservoir 2 is maintained at a constant level. The level of the water in reservoir 1 is initially high so that the fluid in vessel C is water, flowing from 1 to 2. The level of the water in reservoir 1 is allowed to drop slowly as the network drains the reservoir, thus decreasing the pressure at inlet 1. The rate at which the level of reservoir 1 falls is slow compared to the time for the flows to come to equilibrium. At some point we visually observe the flow in C to reverse direction and start flowing from 2 to 1 and we record the water level in reservoir 1. The level of reservoir 1 is then raised by slowly pumping water in such that the bistable region can be confirmed. We find the flow in C remains from 2 to 1 for a sufficiently long time. As the level of reservoir 1 rises, eventually the flow switches direction, back to 1 to 2, and we record the water level in reservoir 1 when this occurs. An example of the experimental path is shown in Figure 2, where our experiment records the two switching points.

We repeat the above experiment for a number of initial sucrose concentrations (viscosities) in reservoir 2. A comparison of the experimental data compared to the model prediction is shown in Figure 3. In general we see good agreement between the model and experiment. For small sucrose concentrations there is no bistable window. As the sucrose concentration (viscosity) exceeds a critical value a bistable window opens up and widens as the sucrose concentration is further increased. The threshold sucrose concentration depends on the specific geometry of the network and is approximately 30% mass fraction for our network, corresponding to $\mu/\mu_{H_2O} = 3$.

The existence of bistability depends on the network geometry and the inlet concentrations or viscosities. It is possible to analytically determine whether a given network and fluid combination can exhibit bistable behavior. The point where the flow in C goes to zero is determined from Eq. 6, $Q_1 R_A = Q_2 R_B$. Our nonlinear equations can be linearized about this point. For simplicity, we assume a mixture that follows the Arrhenius law for viscosity which is a good approximation in our experiments, i.e. $d = 0$ in Eq. 5. Linearizing about the point $Q_C = 0$ yields a criterion for the existence of a cusp, like that seen in Fig. 2. The analysis yields a simple criteria for the existence of bistability,

$$\frac{\mu_2}{\mu_1} \left(\log \left(\frac{\mu_2}{\mu_1} \right) \frac{\rho_1 M_2}{\rho_2 M_1} - 1 \right) > \frac{L_A D_B^4}{L_B D_A^4} + \frac{L_C D_B^4}{L_B D_C^4}. \quad (9)$$

The parameters on the left hand side only depend upon the fluids, while the parameters on the right only depend upon the network geometry. Details of the analysis can be found in the Appendix. If we apply this criteria to our experimental network, we find that $\frac{L_A D_B^4}{L_B D_A^4} + \frac{L_C D_B^4}{L_B D_C^4} = 1.13$, which corresponds to fluid properties for a sucrose solution

with a mass fraction of 29 %; which agrees well with our experimental data. In addition, Eq. 9 also gives a lower bound on the viscosity contrast required to observe bistability. For sucrose solution this value is approximately 2.3.

We also note from Eq. 9 that if we take the limit of the connecting branch C going to zero length, we can still obtain bistability. This limit is the case of two inlets mixing at a point and going to two outlets which is similar to the microfluidic flip-flop studied by Groisman and Quake [3]. Their flip-flop required visco-elastic fluids whereas here we find bistability in a similar geometry with Newtonian fluids only having different viscosities.

Conclusions—We have demonstrated bistability in a simple fluid experiment using two miscible fluids. Typical flow rates for our experiments are such that the maximum Reynolds number in any experiment was around 100 (though typically much less) and laminar flow within the vessels is expected. The only source of nonlinearity is the viscosity of the mixture which is enough to lead to spontaneous flow switching in the network. This prediction is robust and expected to occur in a wide range of fluid systems as a number of mixtures obey the Arrhenius law for viscosity. Although we built a large scale network our predictions are scale free and equally apply to very small and very large vessels as long as the basic assumption of laminar flow is maintained. Obviously more complicated networks with more nodes would be expected to display even more complicated behavior.

It is surprising to us that we can find no evidence that these predictions and experiments have previously been made or carried out. The experiments are simple to perform, the calculations involve elementary mathematics, and the physics has been well-established for over a century. This system also provides a striking example of bistability using equipment which is cheap to buy and fluids that can be prepared at home.

The existence of bistability in this simple network suggests that other networks could be designed and constructed to provide table-top demonstrations of a variety of logic and control devices. These preliminary experiments also don't rule out the possibility of observing dynamic behavior such as spontaneous oscillations. These results may also have relevance for microfluidic applications. In any device with even a simple network involving fluids of different viscosities or concentrated suspensions, we show here that we can not predict the direction of flow in the network without knowing the flow's history.

-
- [1] G. M. Whitesides, *Nature* **442**, 368 (2006).
 - [2] T. Squires and S. Quake, *Reviews of Modern Physics* **77**, 977 (2005).
 - [3] A. Groisman, M. Enzelberger, and S. Quake, *Science* **300**, 955 (2003).
 - [4] A. Groisman and S. Quake, *Physical Review Letters* **92**, 94501 (2004).
 - [5] M. J. Fuerstman, P. Garstecki, and G. M. Whitesides, *Science* **315**, 828 (2007).
 - [6] M. Prakash and N. Gershenfeld, *Science* **315**, 832 (2007).
 - [7] M. Joanicot and A. Ajdari, *Science* **309**, 887 (2005).
 - [8] F. Jousse, R. Farr, D. R. Link, M. J. Fuerstman, and P. Garstecki, *Physical review E, Statistical, Nonlinear, and Soft Matter Physics* **74**, 036311 (2006).
 - [9] M. Schindler and A. Ajdari, *Physical Review Letters* **100**, 1 (2008).
 - [10] M. Belloul, W. Engl, A. Colin, P. Panizza, and A. Ajdari, *Physical Review Letters* **102**, 1 (2009).
 - [11] K. Foster and G. A. Parker, *Fluidics, Components and Circuits* (Wiley-Interscience, London, 1970).
 - [12] A. R. Pries, B. Reglin, and T. W. Secomb, *Hypertension* **46**, 725 (2005).
 - [13] M. A. J. Chaplain, S. R. McDougall, and A. R. A. Anderson, *Annual Review of Biomedical Engineering* **8**, 233 (2006).
 - [14] A. S. Popel and P. C. Johnson, *Annual Review of Fluid Mechanics* **37**, 43 (2005).
 - [15] A. R. Pries, T. W. Secomb, P. Gaehtgens, and J. F. Gross, *Circulation Research* **67**, 826 (1990).
 - [16] R. T. Carr, J. B. Geddes, and F. Wu, *Annals of Biomedical Engineering* **33**, 764 (2005).
 - [17] J. Geddes, R. Carr, N. Karst, and F. Wu, *SIAM Journal on Applied Dynamical Systems* **6**, 694 (2007).
 - [18] L. Grunberg and A. Nissan, *Nature* (1949).
 - [19] D. R. Lide, *CRC Handbook of Chemistry and Physics* (2007).

APPENDIX A: DERIVATION OF BISTABILITY CRITERION

In the text we provide a simple criterion to determine whether a given network and fluid combination can exhibit bistability. In this section we provide a detailed derivation for the interested reader.

The relationship between Q_C and Q_1 was given in the text as,

$$Q_C = \frac{Q_1 R_A - Q_2 R_B}{R_A + R_B + R_C}. \quad (\text{A1})$$

In what follows, it simplifies matters to use the dimensionless flow rate where all flows are scaled by the total flow,

$Q_1 + Q_2$. Under this scaling Eq. 6 becomes,

$$Q_C = \frac{Q_1 R_A - (1 - Q_1) R_B}{R_A + R_B + R_C}, \quad (\text{A2})$$

where for the remainder of this section the Q 's are dimensionless. Note that $Q_1 + Q_2 = 1$. Without loss of generality, in what follows we assume the more viscous fluid is always coming from inlet 2.

1. Equilibrium state

When there is no flow in branch C we have

$$Q_1^* = \frac{R_B^*}{R_A^* + R_B^*}, \quad (\text{A3})$$

and

$$\phi_A^* = 0, \quad \phi_B^* = 1, \quad (\text{A4})$$

where the superscript * refers to the equilibrium solution. We linearize the problem about this point. We expand the solution as $Q_1 = Q_1^* + \delta Q_1$ and $Q_c = \delta Q_C$, where δ denotes this as a perturbation.

2. Positive Q_C

When Q_C is positive (from inlet 1 to inlet 2)

$$\phi_A = 0, \quad \phi_B = \frac{Q_2}{Q_C + Q_2}, \quad \phi_C = 0. \quad (\text{A5})$$

Using our expansion and discarding higher powers of δ yields an expression for ϕ_B ,

$$\phi_B = \frac{1}{Q_C/Q_2 + 1} = \frac{1}{\frac{\delta Q_C}{Q_2^* + \delta Q_2} + 1} = 1 - \frac{\delta Q_C}{Q_2^*} = 1 - \frac{\delta Q_C}{1 - Q_1^*} = 1 - \delta \phi_B \quad (\text{A6})$$

The viscosity of the mixture can be captured using an Arrhenius law,

$$\log(\mu) = (1 - N)\log(\mu_1) + N\log(\mu_2), \quad (\text{A7})$$

where N is the mole fraction of fluid 2. For simplicity of the derivation we discard the empirical parameter d used in the text. The experimental data for the sucrose solutions used in the experiments is well approximated by the standard Arrhenius law. This viscosity equation is equivalent to

$$\frac{\mu}{\mu_1} = \left(\frac{\mu_2}{\mu_1} \right)^N. \quad (\text{A8})$$

The relationship between volume fraction, ϕ , and mole fraction, N , is given as

$$N = \frac{\phi \frac{\rho_2}{M_2}}{\phi \frac{\rho_2}{M_2} + (1 - \phi) \frac{\rho_1}{M_1}} = \frac{1}{1 + \left(1 - \frac{1}{\phi}\right) \frac{\rho_1}{M_1} \frac{M_2}{\rho_2}}. \quad (\text{A9})$$

Thus, expanding about the equilibrium solution for ϕ_B yields,

$$N_B = \frac{1}{1 + \left(1 - \frac{1}{1 - \delta \phi_B}\right) \frac{\rho_1}{M_1} \frac{M_2}{\rho_2}} = \frac{1}{1 - \delta \phi_B \frac{\rho_1}{M_1} \frac{M_2}{\rho_2}} = 1 + \delta \phi_B \frac{\rho_1}{M_1} \frac{M_2}{\rho_2} = 1 + \delta N_B, \quad (\text{A10})$$

and, expanding the viscosity function in the positive flow direction we obtain,

$$\mu_B = \mu_1 \left(\frac{\mu_2}{\mu_1} \right)^{1 + \delta N_B} = \mu_2 \left(1 + \log \left(\frac{\mu_2}{\mu_1} \right) \delta N_B \right). \quad (\text{A11})$$

In terms of the resistance of tube B, we have

$$R_B = \frac{128L_B\mu_2}{\pi D_B^4} \left(1 + \log \left(\frac{\mu_2}{\mu_1} \right) \delta N_B \right) = \frac{128L_B\mu_2}{\pi D_B^4} \left(1 - \frac{1}{1 - Q_1^*} \log \left(\frac{\mu_2}{\mu_1} \right) \frac{\rho_1}{M_1} \frac{M_2}{\rho_2} \delta Q_C \right) = R_B^* - \delta R_B \quad (\text{A12})$$

Now, returning to the original equation for the flow in branch C,

$$Q_C = \frac{Q_1 R_A - (1 - Q_1) R_B}{R_A + R_B + R_C}, \quad (\text{A13})$$

we substitute the solution near the equilibrium point,

$$\delta Q_C = \frac{(Q_1^* + \delta Q_1) R_A^* - (1 - Q_1^* - \delta Q_1) (R_B^* - \delta R_B)}{R_A^* + R_B^* - \delta R_B + R_C^*}, \quad (\text{A14})$$

which linearizes to

$$\delta Q_C (R_A^* + R_B^* + R_C^*) = \delta Q_1 R_A^* + \delta Q_1 R_B^* + (1 - Q_1^*) \delta R_B. \quad (\text{A15})$$

Substituting for δR_B yields,

$$\delta Q_C \left(R_A^* + R_B^* + R_C^* - R_B^* \log \left(\frac{\mu_2}{\mu_1} \right) \frac{\rho_1}{M_1} \frac{M_2}{\rho_2} \right) = (R_A^* + R_B^*) \delta Q_1. \quad (\text{A16})$$

The sign of the slope $\delta Q_C / \delta Q_1$ is given by the sign of expression in parenthesis on the left hand side since the resistances are always positive numbers.

3. Negative Q_C

When Q_C is negative (from inlet 2 to inlet 1),

$$\phi_A = \frac{Q_c}{Q_c - Q_1}, \quad \phi_B = 1, \quad \phi_C = 1. \quad (\text{A17})$$

Using our expansion and discarding higher powers of δ yields an expression for ϕ_A ,

$$\phi_A = \frac{Q_c}{Q_c - Q_1} = \frac{\delta Q_c}{\delta Q_C - Q_1^* - \delta Q_1} = \frac{-\delta Q_c}{Q_1^*} = \delta \phi_A \quad (\text{A18})$$

Expanding about the equilibrium solution for the mole fraction N_A yields,

$$N_A = \frac{\delta \phi_A}{\delta \phi_A + (1 - \delta \phi_A) \frac{\rho_1}{M_1} \frac{M_2}{\rho_2}} = \delta \phi_A \frac{\rho_2}{M_2} \frac{M_1}{\rho_1} = \delta N_A. \quad (\text{A19})$$

The viscosity function near the equilibrium point in the negative Q_C direction is,

$$\mu_A = \mu_1 \left(\frac{\mu_2}{\mu_1} \right)^{\delta N_A} = \mu_1 + \mu_2 \log \left(\frac{\mu_2}{\mu_1} \right) \delta N_A. \quad (\text{A20})$$

In terms of the resistance of tube A, we have

$$R_A = \frac{128L_A\mu_1}{\pi D_B^4} \left(1 + \frac{\mu_2}{\mu_1} \log \left(\frac{\mu_2}{\mu_1} \right) \delta N_A \right) = \frac{128L_A\mu_1}{\pi D_B^4} \left(1 - \frac{\mu_2}{\mu_1} \log \left(\frac{\mu_2}{\mu_1} \right) \frac{\rho_2}{M_2} \frac{M_1}{\rho_1} \frac{1}{Q_1^*} \delta Q_C \right) = R_A^* + \delta R_A \quad (\text{A21})$$

Now, returning to the original equation for the flow in branch C,

$$Q_C = \frac{Q_1 R_A - (1 - Q_1) R_B}{R_A + R_B + R_C}, \quad (\text{A22})$$

we substitute the solution near the equilibrium point,

$$\delta Q_C = \frac{(Q_1^* + \delta Q_1) (R_A^* + \delta R_A) - (1 - Q_1^* - \delta Q_1) R_B^*}{R_A^* + \delta R_A + R_B^* + R_C^*}, \quad (\text{A23})$$

and linearize to obtain,

$$\delta Q_C(R_A^* + R_B^* + R_C^*) = Q_1^* \delta R_A + \delta Q_1 R_A^* + \delta Q_1 R_B^*. \quad (\text{A24})$$

Substituting for the resistance δR_A yields,

$$\delta Q_C \left(R_A^* + R_B^* + R_C^* + R_A^* \frac{\mu_2}{\mu_1} \log \left(\frac{\mu_2}{\mu_1} \right) \frac{\rho_2}{M_2} \frac{M_1}{\rho_1} \right) = \delta Q_1 (R_A^* + R_B^*) \quad (\text{A25})$$

When the flow in C is negative, then the slope at that point of $\delta Q_C / \delta Q_1$ is always positive (we assumed from the start without loss of generality that $\mu_2 > \mu_1$).

4. Bistability

We have linearized our system around the equilibrium point $Q_C^* = 0$. Eqs. A16 and A25 describe the slope of the function $\delta Q_C / \delta Q_1$ at that point. The slope of this curve is discontinuous at this point whenever the viscosities are different. The sign of the slope is always positive when Q_C is negative. When Q_C is positive, the slope can be of either sign according to Eq. A16. Multiple equilibria exist for a given Q_1 if the sign of slope is negative at $Q_C^* = 0$, i.e.

$$\frac{R_A^*}{R_B^*} + 1 + \frac{R_C^*}{R_B^*} < \log \left(\frac{\mu_2}{\mu_1} \right) \frac{\rho_1}{M_1} \frac{M_2}{\rho_2}, \quad (\text{A26})$$

which can be written as

$$\frac{L_A D_B^4}{L_B D_A^4} + \frac{L_C D_B^4}{L_B D_C^4} < \frac{\mu_2}{\mu_1} \left(\log \left(\frac{\mu_2}{\mu_1} \right) \frac{\rho_1}{M_1} \frac{M_2}{\rho_2} - 1 \right). \quad (\text{A27})$$

The terms on the left all depend upon the network geometry where the terms on the right all depend upon the fluid properties. Thus we have a simple criterion for bistability.